Structural basis of the substrate subsite and the highly thermal stability of xylanase 10B from Thermotoga maritima MSB8

ARTICLE *in* PROTEINS STRUCTURE FUNCTION AND BIOINFORMATICS · DECEMBER 2005

Impact Factor: 2.63 · DOI: 10.1002/prot.20700 · Source: PubMed

8 AUTHORS, INCLUDING:

Is Ihsanawati
Bandung Institute of Technology
13 PUBLICATIONS **115** CITATIONS
SEE PROFILE

Takashi Kumasaka
Japan Synchrotron Radiation Research Inst..
144 PUBLICATIONS **6,973** CITATIONS
SEE PROFILE

Tomonori Kaneko
The University of Western Ontario
18 PUBLICATIONS **390** CITATIONS
SEE PROFILE

Rie Yatsunami
Tokyo Institute of Technology
38 PUBLICATIONS **242** CITATIONS
SEE PROFILE

Structural Basis of the Substrate Subsite and the Highly Thermal Stability of Xylanase 10B From *Thermotoga maritima* MSB8

Ihsanawati,[1] Takashi Kumasaka,[1]* Tomonori Kaneko,[1] Chihiro Morokuma,[2] Rie Yatsunami,[2] Takao Sato,[1] Satoshi Nakamura,[2] and Nobuo Tanaka[1]

[1]*Department of Life Science, Tokyo Institute of Technology, Yokohama, Japan*
[2]*Department of Bioengineering, Tokyo Institute of Technology, Yokohama, Japan*

ABSTRACT **The crystal structure of xylanase 10B from *Thermotoga maritima* MSB8 (TmxB), a hyperthermostable xylanase, has been solved in its native form and in complex with xylobiose or xylotriose at 1.8 Å resolution. In order to gain insight into the substrate subsite and the molecular features for thermal stability, we compared TmxB with family 10 xylanase structures from nine microorganisms. As expected, TmxB folds into a $(\beta/\alpha)_8$-barrel structure, which is common among the glycoside hydrolase family 10. The enzyme active site and the environment surrounding the xylooligosaccharide of TmxB are highly similar to those of family 10 xylanases. However, only two xylose moieties were found in its binding pocket from the TmxB-xylotriose complex structure. This finding suggests that TmxB could be a potential biocatalyst for the large-scale production of xylobiose. The result of structural analyses also indicated that TmxB possesses some additional features that account for its thermostability. In particular, clusters of aromatic residues together with a lack of exposed hydrophobic residues are characteristic of the TmxB structure. TmxB has also a significant number of ion pairs on the protein surface that are not found in other thermophilic family 10 xylanases. Proteins 2005;61:999–1009.**

Key words: xylanase; family 10; glycoside hydrolase; *Thermotoga maritima* MSB8; thermostability

INTRODUCTION

Xylanases (β-1,4-D-xylanhydrolase; EC 3.2.1.8) are mainly classified into glycoside hydrolase family 10 or 11[1] on the basis of the amino acid sequences of their catalytic domains. Hydrolysis of the β-1,4-glycosidic bonds of xylan, the major constituent of hemicellulose in the plant cell wall, is important in the paper, food, and animal feed industries. In the paper industry, pollution caused by pulp bleaching under alkaline conditions at high temperature has been minimized by utilizing xylanase instead of organochlorine.[2] Therefore, the discovery of xylanases that are stable at alkaline pH and elevated temperature is of interest from the industrial point of view.

The catalytic domain structures of native and complex forms of family 10 xylanases are available from several microorganisms: *Cellulomonas fimi* (Cfx),[3,4] *Streptomyces lividans* (Slx),[5,6] *Pseudomonas fluorescens* (Pfx),[7–9] *Clostridium thermocellum* (Ctx),[10] *Penicillium simplicissimum* (Psx),[11,12] *Thermoascus aurantiacus* (Tax),[13–15] *Streptomyces olivaceoviridis* (Sox),[16–18] *Streptomyces halstedii* (Shx),[19] and *Geobacillus stearothermophilus* (Gsx).[20,21] The complex structure of family 10 xylanase from *Cellvibrio mixtus*[22] and *Emericella nidulans*[23] have recently been reported. All have similar structures comprising an eight-stranded β/α barrel. Family 10 xylanases perform glycosidic-bond hydrolysis with net retention of anomeric configuration via the double displacement mechanism involving two glutamate residues.[4,6,8] By using a combination of intermediary metabolite and inhibitor complexes and site-directed mutagenesis, the role of each catalytic glutamate has been determined.[4,6,8] The structures of Sox[18] and Pfx,[9] with and without decorated xylooligosaccharide, also reveal the substrate specificity. Despite the well-known biochemical and structural analyses of these enzymes, there is a paucity of information

Abbreviations: Cfx, Xylanase Cex from *Cellulomonas fimi*; Ctx, Xylanase Z from *Clostridium thermocellum*; Gsx, Xylanase T-6 from *Geobacillus stearothermophilus*; Pfx, Xylanase A from *Pseudomonas fluorescens*; Psx, Xylanase A from *Penicillium simplicissimum*; Shx, Xylanase from *Streptomyces halstedii*; Slx, Xylanase A from *Streptomyces lividans*; Sox, Xylanase FXYN from *Streptomyces olivaceoviridis* E-86; Tax, Xylanase from *Thermoascus aurantiacus*; TmxA, Xylanase 10A from *Thermotoga maritima* MSB8; TmxB, Xylanase 10B from *Thermotoga maritima* MSB8; r.m.s.d., Root mean square deviation; ASA, Accessible surface area.

Grant sponsor: National Project on Protein Structural and Functional Analyses, the Ministry of Education, Culture, Sports, Science and Technology of Japan.

Ihsanawati's present address is Protein Research Group, RIKEN Genomic Sciences Center, 1-7-22 Suehiro-cho, Tsurumi-ku, Yokohama, 230-0045, Japan.

Tomonori Kaneko's present address is Department of Biological Sciences, Purdue University, 915 West State Street, West Lafayette IN 47907.

*Correspondence to: Takashi Kumasaka, Department of Life Science, Tokyo Institute of Technology, 4259-B-6 Nagatsuta-cho, Midoriku, Yokohama 226-8501, Japan. E-mail: tkumasak@bio.titech.ac.jp

Received 2 February 2005; Revised 7 June 2005; Accepted 30 June 2005

Published online 24 October 2005 in Wiley InterScience (www.interscience.wiley.com). DOI: 10.1002/prot.20700

TABLE I. Temperature-Based Classification of Family 10 Xylanase[†]

	Sox	Pfx	Slx	Cfx	Shx	*Psx*	*Gsx*	*Ctx*	*Tax*	*TmxB*
Optimum growth temperature (°C)	26	25–30	26–28	30	28–30	*30*	*55*	*60*	*52*	*80*
Optimum temperature for activity (°C)	45	57	60	60	60	*67*	*65*	*70*	*80*	*90*
References	16	13	13	13	20	*11*	*21*	*13*	*13*	*24*

[†]For all of the tables in this article, thermophilic xylanases are in italic while the rest are mesophilic xylanases.

regarding the molecular basis for thermostability of family 10 xylanases. The only thermophilic family 10 xylanase describing its thermal stability mechanism, Tax, has improvements in the hydrophobic packing, favorable interactions of charged side chains with the helix dipoles and the introduction of proline residues at the N-terminus of helices.[15]

Thermotoga maritima MSB8 produces two kinds of thermophilic family 10 xylanases, TmxA and TmxB, which are expressed by two distinct genes, *xynA* and *xynB*, respectively. TmxA is a 120-kDa modular xylanase consisting of five domains, while TmxB is a 38-kDa non modular enzyme composed of a catalytic domain.[24] The most outstanding characteristic of both xylanases is their stability at elevated temperature (~90°C).[24] TmxB is stable at temperatures up to 100°C from pH 7 to 8.5,[25] and is the most stable xylanase among families 10 and 11.[26] We present here the crystal structure of TmxB, the most thermostable xylanase to be structurally characterized. Structural comparison of TmxB with nine other family 10 xylanases (Table I) is used to rationalize the enzymes activity at elevated temperatures.

MATERIALS AND METHODS

Crystallization and Data Collection

Expression and protein purification of TmxB were carried out as reported previously.[27] The best crystals were grown using the hanging drop vapor diffusion method at 25°C by mixing 3 μl of protein solution with 3 μl of reservoir solution containing 0.2 M Li_2SO_4, 0.1 M sodium acetate buffer pH 4.6 and 20% (w/v) PEG 8000. A thin-plate crystal grew to approximately 0.7 mm long in a week.

The complex crystals with xylooligosaccharides were obtained by the soaking method. The soaking solution was prepared by adding each xylobiose or xylotriose in the same reservoir solution containing 30% (w/v) glycerol to a concentration of 25 mg ml^{-1}. The soaking time varied between 5 and 10 min just before applying the crystals into the cryogenic stream.

The diffraction data for native TmxB were collected at SPring-8 on the beamline BL38B1 using an ADSC Quantum detector, while data for TmxB in complex with xylobiose or xylotriose was carried out at Photon Factory PF-AR on the beamline NW-12 using an ADSC 210 detector. Mosflm version 6.2.2[28] was used for data reduction in the *P*1 space group for all of data sets. Integrated intensities were scaled and merged with program SCALA.[28] The reflection intensities were finally converted to structure factor amplitudes with TRUNCATE.[28]

Structure Solution and Refinement

The native TmxB structure has been determined by the molecular replacement method using the program Molrep in the CCP4 suite,[28] which was carried out with data from 10 to 4 Å resolution by taking the catalytic domain structure of the family 10 xylanase, Ctx[10] as a search model. After the initial refinement of the model with the data within 2.5 Å resolution, the maximum-likelihood simulated annealing protocol of CNS program[29] was applied for the refinement of the model with the data within 1.8 Å resolution. A subset of 5% of the data set was used for cross-validation R_{free} calculations. All model building works were performed with XtalView program.[30] Water molecules were added automatically with the CNS program[29] and inspected manually with the $2F_o$-F_c and F_o-F_c maps. After several cycles of refinement, heterocompounds such as sulfate and acetate ions were added.

The refined native TmxB structure was then used as the model to determine the complex structure of TmxB with 1.8 Å resolution. Ten percent of observations were used as the R_{free} set in the refinement of each TmxB-complex structure. The stereochemistry validation of all structures was performed with PROCHECK.[31] Data collection and refinement statistics are given in Table II.

Reaction Product Assay

Thin-layer chromatography (TLC) was performed on a microcrystalline cellulose TLC plate (Merck) to analyze the reaction product of TmxB-xylotriose as described previously.[32] The reaction was initiated by mixing 30 mg ml^{-1} TmxB with 25 mg ml^{-1} xylotriose in 10 mM MES buffer pH 6.0 at room temperature. An aliquot of the reaction mix was taken at selected intervals and spotted onto a TLC plate. The plate was developed twice in an ethanol/acetic acid/water (ratio 3:2:1, respectively) solvent system. Xylotriose hydrolysate was detected by heating the TLC plate for a few minutes in a hot dry oven after dipping the plates in the aniline-hydrogen phthalate reagent. A solution mixture containing xylose, xylobiose, and xylotriose (Wako, Japan) was used as the standard.

Software Used for Structural Analyses

Amino acid compositions and alignments of family 10 xylanases were calculated with the ProtParam software in ExPASy proteomics server[33] and the ClustalW,[34] respectively. The Top3d program implemented in CCP4 suite[28] calculates the r.m.s.d. between structures after fitting. A comprehensive molecular analysis of each protein structure was also obtained by employing DSSP[35] (secondary structure compositions and total number of hydrogen

TABLE II. Data Collection and Refinement Statistics[†]

Parameters	Native	Xylobiose	Xylotriose
Data collection			
X-ray source	SPring-8 BL38B1	PF-AR NW12	PF-AR NW12
Space group	*P*1	*P*1	*P*1
Cell dimensions *a* (Å); α (°)	58.50; 84.59	58.29; 84.49	58.44; 84.27
b (Å); β (°)	59.10; 71.14	58.78; 71.13	58.60; 70.46
c (Å); γ (°)	61.34; 68.32	61.00; 68.55	61.11; 68.76
Resolution range (Å) (high-resolution shell)	57–1.8 (1.87–1.80)	30–1.8 (1.87–1.80)	30–1.8 (1.87–1.80)
R_{merge} (%)[a]	7.8 (27.9)	4.1 (17.7)	5.6 (28.3)
Completeness (%)	99.9 (99.9)	97.4 (97.4)	96.7 (96.7)
Mean I/σ_I	6.6 (2.7)	13.8 (4.3)	6.7 (2.6)
Refinement			
R_{factor}/R_{free} (%)[b]	19.15/21.99	18.33/21.62	20.27/22.94
Average B-factor (Å^2)	12.02	19.22	17.98
r.m.s.d. bonds (Å)	0.005	0.005	0.005
r.m.s.d. angles (°)	1.319	1.287	1.303
Ramachandran Plot %-residue in the most favored region	89.6	89.9	89.1
%-residue in add. allowed region	10.4	10.1	10.9
%-residue in gen. allowed region	0	0	0
%-residue in disallowed region	0	0	0
PDB code	1VBU	1VBR	—

[†]Values in parentheses are for the highest resolution shell.
[a]$R_{merge} = \Sigma_{hkl} \Sigma_i |I_{hkl,i} - \langle I_{hkl} \rangle| / \Sigma_{hkl} \langle I_{hkl} \rangle$.
[b]$R_{factor} = \Sigma ||F_{obs}| - |F_{calc}|| / \Sigma |F_{obs}|$.

bond), Vadar[36] (ion pairs, ASA total, and ASA hydrophobic residues), and Areaimol[28] (ASA of an individual residue). VOIDOO[37] was used to compute cavity and molecular protein volumes with a probe radius of 1.4 Å and without a probe. Solvent molecules and heterocompounds are omitted for these calculations. Figures were prepared using MOLSCRIPT,[38] Raster3D,[39] ESPript version 2.2,[40] and Pymol.[41]

RESULTS AND DISCUSSION

Overall Structure

The structure of TmxB has been determined at 1.8-Å resolution for the native enzyme and ternary complex with either xylobiose or xylotriose (Table II). All structures belong to the space group *P*1 containing two xylanase molecules, each of which is composed of 324 residues. The r.m.s.d. values calculated for all the Cα atoms is 0.13 Å by fitting two crystallographically independent molecules in either native or complex structures. Three residues at the N-terminus and one residue at the C-terminus in each molecule are missing in the electron density maps of all structures. A Ramachandran plot confirmed the stereochemical validity where all residues are in allowed regions with acceptable values of bond angle geometry (Table II).

TmxB folds into an eight-stranded β/α barrel (TIM-barrel)[42] structure [Fig. 1(A)], which is similar to other family 10 glycoside hydrolases. It is composed of eleven β-strands and fourteen α-helices including one 3_{10}-helix (residue 538–540). The β-sheet structures consisting of eight parallel β-strands (green) lie in the middle forming a barrel surrounded by eight α-helices (red) with an elliptical size of 55 × 43 × 40 Å^3 [Fig. 1(A)]. Additional secondary structures including the 3_{10}-helix structure are on the top of barrel. This β-barrel is composed of many hydrophobic residues that interact closely with other hydrophobic residues from adjacent α-helices at the core of the enzyme. A long groove exists at the top of the β-barrel structure where two catalytic residues, Glu647 and Glu753, are located. The groove is at the C-terminal end of the β-barrel and exposed to the surface. This generates a space for the two xylose units to bind the catalytic pairs [Fig. 1(A)].

Binding of Xylooligosaccharide to the Active Site

The complex structures of TmxB show the xylooligosaccharides bind to the catalytic residues (Glu647 and Glu753). Glu753 is located in a cluster of charged residues (Arg656 and His598) and may carry a partial negative charge judging from the hydrogen bonding with $N\epsilon_2$ of His724 (3.50 Å) and $N\delta_2$ of Asn688 (3.03 Å), both of which possess a partial positive charge. The role of Glu753 in catalysis has been demonstrated by mutational analysis of Pfx where the corresponding glutamate residue was mutated to Ala (E246A) resulting in a complete loss of activity.[8] The acid-base residue, Glu647, is stabilized by hydrogen bonding its $O\epsilon_1$ with $N\epsilon_1$ of Trp602 (3.40 Å) and its $O\epsilon_2$ with $N\epsilon_2$ of Gln722 (2.90 Å), respectively. These catalytic residues and residues in the vicinity of the catalytic site are highly conserved in the family 10 xylanases as shown previously.[4–8,22]

The structure found in other family 10 xylanase complex structures was not observed in TmxB due to the inverse conformation of the second xylose [Fig. 1(B)]. Although two

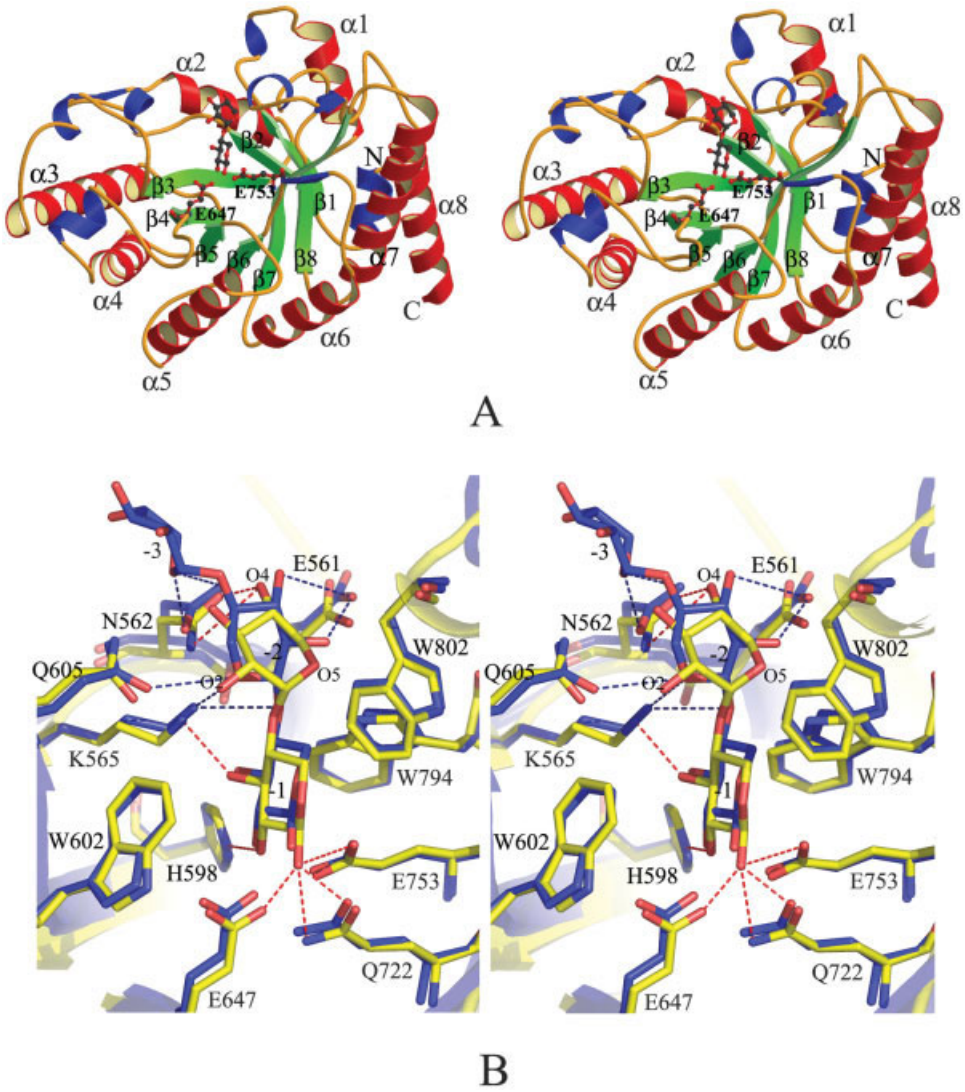

Fig. 1. **A:** Overall structure of TmxB (in stereo) from the top view. Major α-helices and β-strands are drawn in red and green, respectively, and labeled according to the ideal $(\beta/\alpha)_8$ barrel structure.[42] The two catalytic residues are labeled and depicted by *ball-and-stick* facing two xylose moieties. **B:** Stereo view of superimposition of TmxB-xylotriose (yellow) with Psx-xylotriose (blue) in the catalytic site. Red dash lines indicate hydrogen bonds in the TmxB complex structure, which are also found in Psx. Blue dash lines represent hydrogen bonds, which are only found in Psx.

rings of xylobiose and xylotriose were found in the region referred to as subsite −1 and −2 in the electron density map of the complex structures of TmxB, the third xylose moiety of xylotriose was missing at subsite −3. This numbering system follows the nomenclature for sugar-binding subsites in glycoside hydrolases.[43] The xylose unit at subsite −1 adopts a chair conformation and has van der Waals interactions with Trp602, Trp802, and Trp794. It has also some hydrophilic interactions via O_1, O_2, and O_3 with the enzyme [Fig. 1(B)]. The O_1 forms hydrogen bonds with $O\epsilon_2$ of Glu647 (2.32 Å) and Glu753 (3.41 Å), $O\epsilon_2$ and $N\epsilon_2$ of Gln722 (2.94 and 2.58 Å), respectively. The O_2 interacts with $N\epsilon_2$ of His598 in a distance of 2.99 Å and the O_3 forms hydrogen bonds with Nζ of Lys565 (2.64 Å) and all of which are highly similar to other family 10 xylanases [Fig. 1(B)]. However, the conformation of TmxB xylose at subsite −2 is different from other family 10 xylanases because the O_5 and C_2 of the xylose moiety is rotated by 180° along the C_1–O_1 connection [Fig. 1(B)]. This rotation prevents any hydrophilic interaction of xylose at subsite −2 with Gln605, Lys565, and Glu561, and subsite at −3 with $O\delta_1$ and $N\delta_2$ of Asn562 as shown by blue dash lines in Figure 1(B). When the structure of TmxB-xylotriose was superimposed with that of Psx-xylotriose,[12] the third xylose ring of TmxB does not interact with the enzyme by neither electrostatic nor van der Waals interactions. In contrast, the corresponding xylose of Psx interacted weakly with residues surrounding the catalytic site [Fig. 1(B)] via hydrogen bonds with $O\delta_1$ and $N\delta_2$ of Asn48 (equivalent to Asn562 in TmxB).

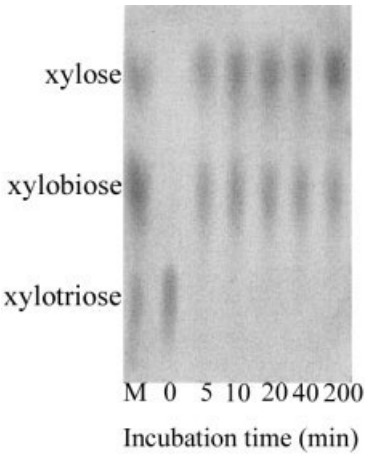

Fig. 2. A thin layer chromatogram of xylotriose hydrolysate. Xylotriose was incubated with the same concentration of TmxB used for crystallization at room temperature. Lane M is a marker consisting of xylose, xylobiose, and xylotriose. Lane 0 consists of xylotriose before reaction. Lane 5, 10, 20, 40, and 200 indicates the incubation time (minutes).

The hydrolysis of xylotriose into xylobiose and xylose by TmxB during the soaking process was shown by thin layer chromatographic analysis (Fig. 2). Reaction temperature and concentration of the enzyme were adjusted with the condition of the crystal soaking into the xylotriose solution. Within 5 min, the band corresponding to xylotrioses disappeared as shown in Figure 2. This result is consistent with the crystallographic data in which no residual electron density hump is observed in the difference map of TmxB-xylotriose. The previous biochemical analysis of xylanase 10B also suggested that TmxB decomposes xylooligosaccharides to yield predominantly xylobiose and a small amount of xylose.[25,44] This result is likely to indicate that TmxB is a potential biocatalyst for the large-scale production of xylobiose.

Comparison of TmxB With Family 10 Xylanases: General Adaptation to High Temperature

The increasing number of crystal structures between thermophilic and mesophilic proteins in the same family have been used to rationalize several structure properties that may be responsible for thermostabilizing factors. However, this is still a matter of controversy and no general strategy has yet been obtained to increase stability of mesophilic proteins into thermophilic ones. TmxB has an optimum temperature for the activity at 90°C and is still active at 105°C.[24] Indeed, TmxB is the most thermostable enzyme among nine members of family 10 xylanases used in this study (Table I).

The sequence alignment and overall superimposition of Cα atoms of TmxB and nine members of family 10 xylanases are presented in Figure 3 and Table III, respectively. The position of Cα atoms of all the catalytic domain structures of family 10 xylanases shows that TmxB is superimposed well with the others giving the r.m.s.d. in the range of 0.89–1.17 Å. However, their thermostabilities differ evidently. The amino acid sequence of TmxB shares the identity with the others in the range of 38–46% (Table III). The most highly conserved amino acids constitute the active site of the protein, which is an open deep cleft at the C-terminal region of the β-strands indicated by red and red-blocked characters in Figure 3. The less well-conserved region of the protein is likely to play an important role in explaining why TmxB has a high adaptation to the elevated temperature.

Primary and Secondary Structural Comparison

Genome analysis in many thermophilic enzymes showed that amino acid composition is considered to be correlated to the protein thermostability.[45,46] Comparison of the amino acid composition of TmxB with other family 10 xlanases displays some interesting differences, yet their secondary structure are strikingly similar (Table IV). TmxB contains the lowest number of residues that are decomposed easily (Ser and Thr, 7.4%) and thermolabile residues (Asn and Gln, 7.8%) as well as a relatively small number of Met (1.9%) and Cys (0.9%), which are easily oxidized at the high temperature among family 10 xylanases (Table IV). Structurally, comparison showed that Met and Cys residues of TmxB are relatively buried inside the structure compared with other family 10 xylanases, to resist from being oxidized easily at a high temperature. Reducing the number of amino acids that are easily deaminated and oxidized at a high temperature in TmxB is consistent with the structural analysis of some hyperthermophilic enzymes.[45–48]

Proline residues at suitable positions have been reported to enhance the protein thermostability by controlling protein folding due to their rigid conformations that can restrict the main chain flexibility of the protein structures.[47] TmxB has 3.7% of proline, which is more than the average of mesophiles, although it is less than the average of thermophiles. Most of the proline residues in TmxB are in loops and α-helices structures that are not conserved in the family 10 xylanases, and thus might help TmxB to keep its folding at the high temperature. Of the five Pro residues found in helices, three of them are at the N1 position. They are Pro607, Pro666, and Pro824 (Fig. 3). A kink in the peptide backbone introduced by a proline residue at the N1 position is reported to stabilize the α-helix thermodynamically.[47]

Disulfide bridges as stabilizing and catalytic structure elements seem to be more abundant in proteins from hyperthermophiles.[48] TmxB and Ctx have three and six cysteines, respectively. However, none of them form a disulfide bond compared with other family 10 xylanase. Indeed, Ctx has two adjacent cysteines, connecting the end of α-helix 7 and β-strand 8, where two Sγ have been separated more than 5 Å. Six members of family 10 xylanases (Sox, Slx, Shx, Cfx, Tax, and Psx) have a disulfide bridge at the related position. However, TmxB does not have a disulfide bridge at this position due to valine (Val788) instead of cysteine on β-strand 8 (Fig. 3). Cys775 and Cys825 of TmxB are close to each other but their Sγ atoms are separated by 4.47 Å. Probably, disulfide bridges are not the major thermostabilizing factors for *T. maritima* proteins. Lactate dehydrogenase from *T. mari-*

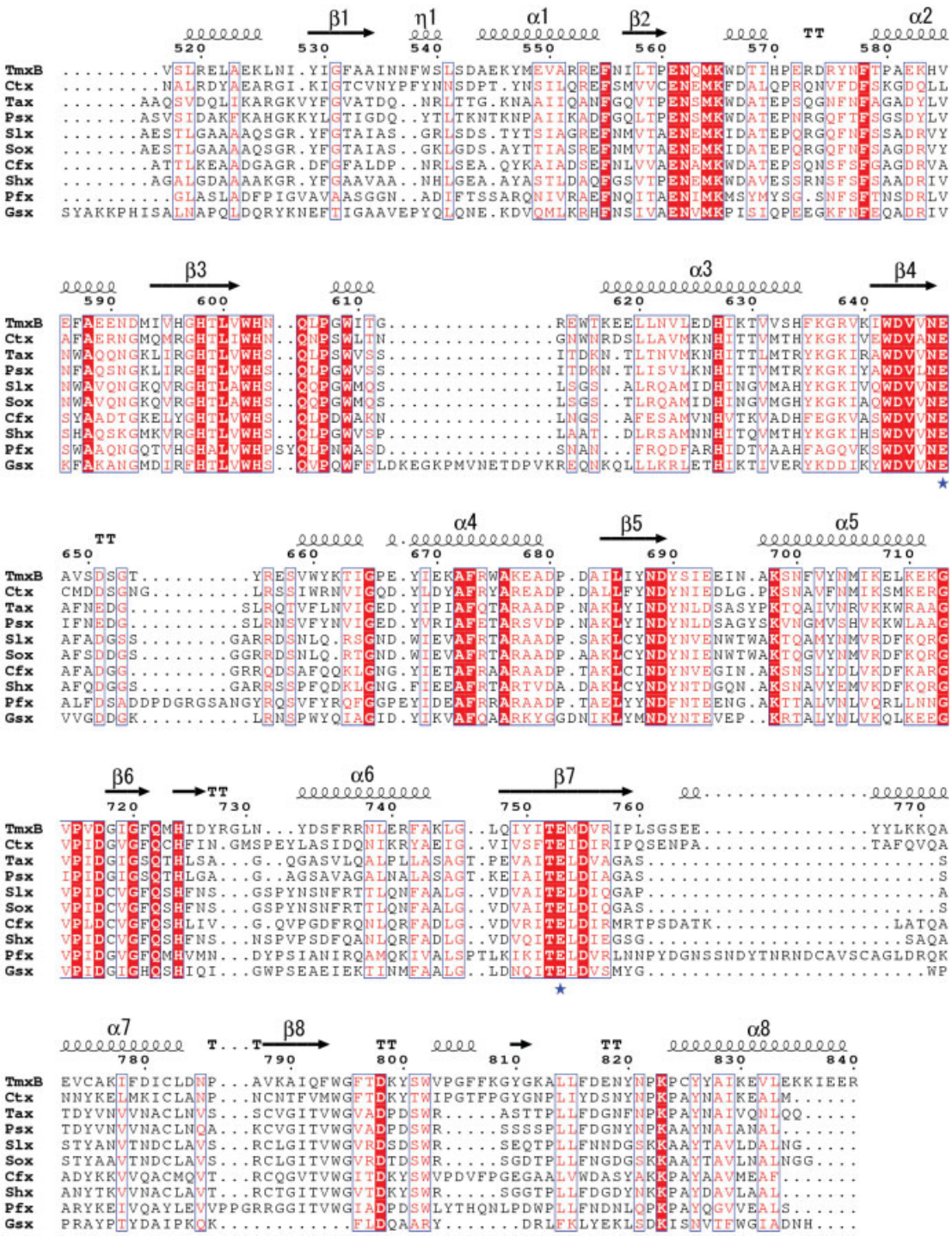

Fig. 3. Sequence alignment of family 10 xylanases. Secondary structures are labeled according to the ideal $(\beta/\alpha)_8$ barrel structure.[42] Red and red-blocked characters indicate conserved and highly conserved residues surrounding the active site, respectively. Blue stars indicate the catalytic pair. The sequence number is based on TmxB.

tima, which has thermal denaturation at 91°C, does not adapt the disulfide bridge as its thermal stabilizing mechanism.[49]

Aromatic Cluster

The aromatic cluster is one type of hydrophobic interaction that has been calculated to have non-bonded potential energies between 1 and 2 kcal mol^{-1}.[50] The closely packed aromatic residues may play an important role in stabilizing the enzyme at high temperature as found with hyperthermophilic organisms in previous reports.[51–54] TmxB has the most abundant aromatic residues (14.2%) among family 10 xylanases. There are five aromatic clusters in

TABLE III. Superimposition of TmxB With Other Family 10 Xylanase Structures

Parameter	Sox	Pfx	Slx	Cfx	Shx	*Psx*	*Gsx*	*Ctx*	*Tax*	*TmxB*
Σ amino acids calculated for	303	312	302	345	302	*301*	*318*	*302*	*320*	*324*
Amino acid identity (%)	41.1	41.8	41.1	41.8	45.0	*38.9*	*39.8*	*46.3*	*39.5*	—
Cα-matching residues	280	297	280	273	278	*265*	*254*	*307*	*266*	—
PDB native	1XYF[16]	1CLX[7]	1E0W[5]	2EXO[3]	1NQ6[19]	*1BG4*[11]	*1HIZ*[20]	*1XYZ*[10]	*IIIW*[13]	*1VBR*
rmsd native	0.91	1.17	0.91	0.91	0.86	*1.03*	*1.03*	*0.89*	*1.00*	—
PDB complex[a]	1ISW[17]	—	1E0X[6]	1FH7[4]	—	*1B3W*[12]	—	—	*1GOR*[14]	*1VBU*
rmsd complex	0.95	—	0.91	0.97	—	*1.02*	—	—	*1.01*	—

The italic characters in the columns of space group is a nomenclature of crystallography.
[a]Complex with xylobiose or its related compounds.

TABLE IV. Differences in the Amino Acid and the Secondary Structure Compositions Among Family 10 Xylanases (%)[†]

Parameters	Sox	Pfx	Slx	Cfx	Shx	Meso	Psx	Gsx	Ctx	Tax	TmxB	Thermo
Alanine	11.6	11.0	12.3	**14.4**	13.2	12.5	*11*	*6.9*	*6.9*	*11.6*	***6.2***	*8.5*
Valine	6.3	7.2	6.6	**8.7**	7.9	7.3	*7.0*	*6.3*	***5.0***	*8.6*	*6.5*	*6.7*
Leucine	**5.3**	6.7	**5.3**	6.1	5.6	5.8	***7.3***	*6.9*	*5.9*	***7.3***	*6.8*	*6.8*
Isoleucine	4.0	4.6	3.6	2.6	**2.6**	6.4	*7.0*	*7.5*	*7.2*	*5.6*	***8.0***	*7.1*
Methionine	2.0	1.7	2.3	1.6	1.7	1.9	***1.0***	*2.2*	***4.1***	*1.0*	*1.9*	*2.0*
Proline	**2.0**	4.9	2.3	3.2	3.0	3.1	*3.0*	***5.0***	***5.0***	*4.3*	*3.7*	*4.2*
Tryptophan	3.0	**2.0**	3.0	2.2	**2.0**	2.4	*2.3*	*2.2*	*2.2*	*2.6*	***3.1***	*2.7*
Phenylalanine	4.0	4.3	4.0	5.1	4.6	4.4	*3.0*	*4.1*	*5.0*	***3.0***	***5.2***	*4.1*
Tyrosine	3.3	4.3	3.3	3.2	3.3	3.5	*4.3*	*5.0*	*5.6*	***3.0***	***5.9***	*4.8*
Cysteine	**1.3**	0.6	**1.3**	**1.3**	**1.3**	1.1	*0.7*	*0*	*1.9*	*0.7*	*0.9*	*0.8*
Glycine	**10.2**	7.0	7.9	7.7	8.6	8.3	*8.6*	***5.0***	*6.2*	*7.0*	*5.2*	*6.4*
Serine	7.9	7.0	8.9	5.4	8.3	7.5	***8.6***	*3.5*	*5.0*	*6.6*	***4.0***	5.5
Threonine	6.9	4.1	6.0	4.8	5.3	5.4	*6.3*	*3.5*	*4.1*	*7.3*	***3.4***	*4.9*
Asparagine	6.9	8.4	7.3	4.5	5.6	6.5	*8.0*	*6.0*	***10.3***	*8.3*	***5.9***	*7.7*
Glutamine	5.3	5.2	5.6	4.5	4.3	5.2	*2.3*	***6.0***	*3.8*	***6.0***	***1.9***	*4.0*
Aspartic acid	6.6	7.2	6.3	**8.3**	7.3	7.1	*6.0*	*6.9*	*6.2*	***5.6***	***5.6***	*6.1*
Glutamic acid	3.0	3.5	3.3	4.5	3.3	3.5	*2.7*	*6.9*	*5.0*	***2.3***	***10.5***	*5.5*
Arginine	5.6	5.5	**6.0**	4.5	4.3	5.2	***2.3***	*4.1*	*4.4*	*3.3*	*4.6*	*3.7*
Lysine	3.3	**2.6**	3.0	5.8	5.0	3.9	*6.6*	***9.4***	*4.7*	*4.6*	*8.3*	*6.7*
Histidine	1.7	2.0	1.7	1.6	**2.6**	1.7	*2.0*	*2.5*	*1.6*	***1.3***	*2.5*	*2.0*
Σ Hydrophobic residues[a]	**38.2**	42.4	39.4	43.9	40.6	40.9	*41.6*	*41.1*	*41.3*	***44***	*41.4*	*41.9*
Σ Aromatic residues[b]	10.3	10.6	10.3	10.5	9.9	10.3	*9.6*	*11.3*	*12.8*	***8.6***	***14.2***	*11.3*
Σ Charged residues[c]	20.2	20.8	20.3	24.7	22.5	21.7	*19.6*	*29.8*	*21.9*	***17.10***	***31.5***	*24.0*
Ser+ Thr	14.8	11.1	14.9	10.2	13.6	12.9	***14.9***	*7.0*	*9.1*	*13.9*	***7.4***	*10.4*
Asn+Gln	12.2	13.6	12.9	9.0	9.9	11.5	*10.3*	*12.0*	*14.1*	***14.3***	***7.8***	*11.7*
α-helix	42	45	43	42	41	42.6	*41*	***38***	*46*	*45*	***46***	*43.2*
β-strand	20	20	**22**	20	**22**	20.8	*21*	*20*	***17***	*18*	*20*	*19.2*
Σ secondary structure	62	65	65	62	63	63.4	*62*	***58***	*63*	*63*	***66***	*62.4*

[a]A, F, W, M, V, I, L, and P.
[b]F, Y, and W.
[c]E, D, R, K, and H.
[†]The highest and the lowest values are in bold. The averaged value of mesophilic and thermophilic xylanases is represented by meso and thermo, respectively.

TmxB that account for 38 of the 46 aromatic residues (Table IV) as shown by different colors in Figure 4(A). All of the clusters are within a side chain distance (<7 Å) and orientated with the phenyl ring angle of <90°.[51] Most of the aromatic interactions appear in the loop and helix regions between buried or partially buried residues. Cluster I (orange) contains a large number of aromatic residues stacked closely around the N- and C-terminal regions connecting α1, α2, β1, and β8. Cluster II (green), which is made up of 4 aromatic residues, is in the loop region connecting α2 and α3. Long aromatic connections appear in cluster III (yellow), started from α3 to α5 with tryptophan and phenylalanine as the major aromatic residues. This cluster seems to stabilize the inner part of the helix barrel. Cluster IV (cyan) joins α5 and α6, which consists of 3 phenylalanine and 2 tyrosine residues. The last cluster (blue) connects aromatic residues in β7 and α7 and loop β8α8. All aromatic clusters in TmxB are proposed to play

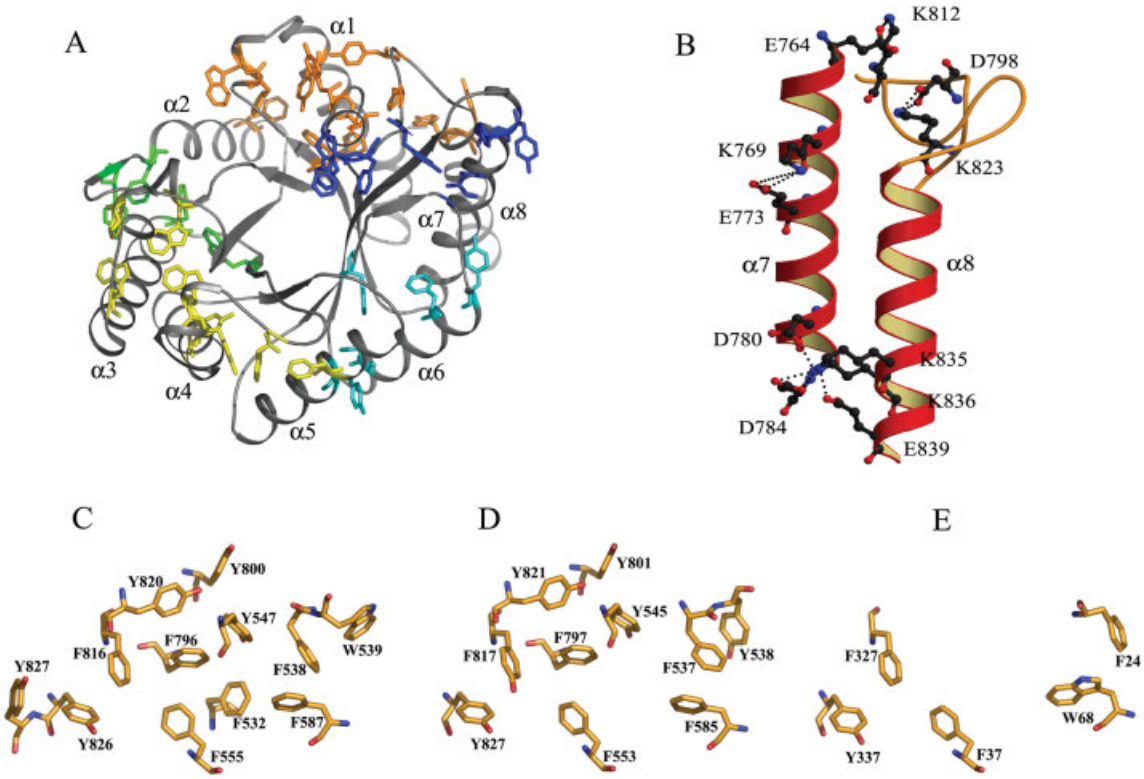

Fig. 4. Molecular interactions for thermal stability of TmxB. **A:** Aromatic interactions from the top view showing five distinct clusters drawn in different colors. **B:** Electrostatic interactions in the C-terminal region consist of a triad salt bridge (Asp780-Asp784-Lys836) and single ones (Lys769-Glu773, Asp798-Lys823 and Lys835-Glu839. **C–E:** Comparison of aromatic interactions, connecting α1, α2, β1, and α8 in TmxB, Ctx, and Pfx, respectively.

an important role in stabilizing the loops and inner helix structures. The distribution of aromatic residues of TmxB (hyperthermophile), Ctx (thermophile), and Pfx (mesophile) in the area connecting α1, α2, β1, and α8 were compared with each other [Fig. 4(C–E)]. The aromatic cluster in the same area of TmxB is separated into two parts in Ctx due to the fewer number of aromatic residues (12.8%) [Fig. 4(D)]. Interestingly, the aromatic amino acids of mesophilic Pfx are distributed widely to form small clusters [Fig. 4(E)], despite an abundance of aromatic residues (10.6%) in this enzyme (Table IV).

Hydrogen Bonds and Ion Pairs

Despite similar content of total hydrogen bonds with nine members of family 10 xylanases, TmxB has more charged residues (Table IV) and possible salt bridges (Table V). Most of charged residues and salt bridges found in TmxB are not conserved within the family 10 xylanases. There are two types of ion pair interactions found in TmxB [represented in Fig. 4(B)], one of which is a single salt bridge between positive and negatively charged residues, and the other is a triad salt bridge between three charged residues (i.e., two negative and one positive charge or vice versa). The triad salt bridge contribute the free energy of more than 1 kcal mol^{-1} in excess of the sum of the single salt bridge.[55] TmxB possesses six triad salt bridges in which five of them are not found among other family 10 xylanases. These are Glu625-Lys629-Glu768, Asp780-Asp784-Lys836, Lys617-Glu667-Lys671, Asp651-Lys689-Lys698, and His596-His598-Asp643. A salt bridge of Glu582-His634-Arg638 is found in other family 10 xylanases. Salt bridges and ion pairs of TmxB appear on the surface of the molecule stabilizing mostly the outer helices and loop regions, thus giving significant value of exposed charged ASA (Table V). The salt bridges that stabilize α-helices 7 and 8 as shown in Figure 4(B) are not conserved among family 10 xylanases except for D798-K823, which is found in all family 10 xylanases. Consistent with other hyperthermophilic proteins, abundance of salt bridges especially the triad one contributes to increase the protein stability.[56,57] However, the salt bridge is not found as a major stabilizing interaction for thermophilic family 10 xylanases.[15] Surprisingly, other thermophilic enzymes, such as Psx, Gsx, Ctx, and Tax, possess only 18 salt bridges compared with 20 for the mesophilic xylanases (Table V). Moreover, structural analysis showed that exposed charged ASA of thermophilic xylanase excluded TmxB is similar to that of mesophilic counterpart (Table V). Therefore, the role of salt bridges for thermal stabilizing of the family 10 xylanases remains to be investigated.

Molecular Packing

The accessible surface area of TmxB is relatively greater than those of mesophilic family 10 xylanase. However, only 15.8% of its hydrophobic residues are located at the accessible surface region (Table V). The majority of the

TABLE V. Salt Bridge and Hydrophobic Packing Comparison of Family 10 Xylanase

Parameters	Sox	Pfx	Slx	Cfx	Shx	Meso	Psx	Gsx	Ctx	Tax	TmxB	Thermo
Hydrogen bonds (%)	71.0	67.2	70.2	74.0	74.2	*71.32*	*71.1*	*72.6*	***74.4***	*72.5*	*73.5*	*72.82*
Salt bridges	20	19	21	20	22	20.4	*18*	*19*	*19*	***15***	***29***	*20*
Total atoms for volume calculation	2,319	2,700	2,385	2,400	2,300	—	*2,298*	*2,615*	*2,583*	*4,538*	*2,703*	—
ASA ($\times 10^3$ Å^2)	10.94	13.52	11.51	11.89	11.33	11.85	***10.80***	***15.56***	*12.77*	*11.14*	*13.66*	*12.80*
Volume ($\times 10^4$ Å^2)	5.32	6.31	5.57	5.59	5.37	5.63	***5.29***	***6.39***	*6.08*	*5.40*	*6.35*	*5.90*
Σ cavity (volume Å^3)	—	1 (8.48)	1 (4.32)	1 (12.97)	1 (7.34)	—	*1 (5.37)*	—	—	—	—	—
Packing density[a]	0.566	0.556	**0.616**	0.559	0.558	0.571	*0.571*	***0.537***	*0.559*	*0.573*	*0.559*	*0.560*
Void Volume/atom[b]	**11.66**	10.39	10.42	10.27	10.30	10.55	*9.43*	*10.92*	*10.37*	***5.30***	*10.34*	*9.27*
Hydrophobic ASA (%)	17.25	23.88	20.28	24.31	19.15	20.97	*20.72*	*16.89*	***24.52***	*23.73*	***15.75***	*20.32*
Exposed charged ASA (%)	14	12	15	17	16	14.8	*11*	*21*	***16***	*11*	***27***	*17.2*

[†]The highest and the lowest values are in bold. The averaged value of mesophilic and thermophilic xylanases is represented by meso and thermo, respectively.
[a]Ratio of Van der Waals volume with a probe of 0 and 1.4 Å.
[b]Substraction of Van der Waals volume with a probe of 1.4 and 0 Å per atoms.

hydrophobic residues are buried where they help to form a compact stable protein structure. A paucity of hydrophobic residues exposed at the protein surface is generally associated with extreme thermophilicity.[26,53–57]

An assembly of different interactions contributes to increasing the compactness of the enzyme by reducing the number and volume of cavities inside the protein.[51] The total packing density and void volume per atom of family 10 xylanases, calculated with the program VOIDOO,[36] indicates that the mesophilic enzyme Slx has the highest packing density and a moderately lower void volume (Table V). TmxB has a lower packing density and a similar void volume. Other thermophilic xylanases also have a lower packing density than those of mesophilic xylanases and do not have cavities inside their structures. There is no clear tendency of packing density and void volume for TmxB and other thermofilic proteins of family 10 xylanases. Therefore, the compact structure of the highly thermostable TmxB may result from accumulation of hydrophobic residues and no cavity inside the structure.

CONCLUSIONS

A xylanase from *Thermotoga maritima* MSB8 is a hyperthermophilic enzyme from glycoside hydrolase family 10, which has a TIM-barrel structure. TmxB has the active site and environment surrounding bound xylooligosaccharide similar to the enzymes in the same family. There are only two xylose moieties at the subsite −2 and −1 in the binding pocket deduced from the enzyme-complex crystal structures. The catalytic activity of TmxB forming xylobiose was tested by using a thin layer chromatography. Therefore, TmxB hydrolyzed xylotriose into xylobiose and xylose in the crystal and in the solution states, thus giving a possibility to be used as a potential biocatalyst for the large-scale production of xylobiose.

Compared with enzymes in the same family from nine microorganisms, the structure of TmxB is thermally stabilized by accumulation of several interactions inside and on the surface of the molecule. Aromatic clusters which are partially buried inside the barrel structure, few hydrophobic residues are exposed to the protein surface, and no cavities are proposed to stabilize the inner structure. A significant number of salt bridges, ion pairs, and hydrogen bonds are likely to stabilize the outer helices and loop regions of the TmxB structure. A small number of amino acids that are easily decomposed, deaminated, and oxidized at high temperature probably also contribute to the thermal stability of TmxB.

ACKNOWLEDGMENTS

We thank the BL-38B1 beam line support staffs in SPring-8 and the NW-12 beam line staff in PF-AR.

REFERENCES

1. Henrissat B, Bairoch A. New families in the classification of glycoside hydrolases based on amino acid sequence similarities. Biochem J 1993;293:781–788.
2. Viikari L, Kantelinen A, Sundquist J, Linko M. Xylanases in bleaching: from an idea to the industry. FEMS Microbiol Rev 1994;13:335–335.
3. White A, Withers SG, Gilkes NR, Rose DR. Crystal structure of the catalytic domain of the β-1,4-glycanase Cex from *Cellulomonas fimi*. Biochemistry 1994;33:12546–12552.
4. White A, Tull D, Johns K, Withers SG, Rose DR. Crystallographic observation of a covalent catalytic intermediate in a β-glycosidase. Nat Struct Biol 1996;3:149–154.
5. Derewenda U, Swenson L, Green R, Wei Y, Morosoli R, Shareck F. Crystal structure, at 2.6 Å resolution, of the *Streptomyces lividans*

xylanase A, a member of the F family of β-1,4-β-glycanases. J Biol Chem 1994;269:20811–20814.
6. Charnock SJ, Spurway TD, Xie H, Beylot MH, Virden R, Warren RA, Hazlewood GP, Gilbert HJ. The topology of the substrate binding clefts of glycoside hydrolase family 10 xylanases are not conserved. J Biol Chem 1998;273:32187–32199.
7. Harris GW, Jenkins JA, Connerton I, Pickersgill RW. Refined crystal structure of the catalytic domain of xylanase A from *Pseudomonas fluorescens* at 1.8 Å resolution. Acta Crystallogr D Biol Crystallogr 1996;52:393–401.
8. Harris GW, Jenkins JA, Connerton I, Cummings N, Lo Leggio L, Scott M, Hazlewood GP, Laurie JI, Gilbert HJ, Pickersgill RW. Structure of the catalytic core of the family F xylanase from *Pseudomonas fluorescens* and identification of the xylopentaose-binding sites. Structure 1994;2:1107–1116.
9. Pell G, Szabo L, Charnock SJ, Xie H, Gloster TM, Davies GJ, Gilbert HJ. Structural and biochemical analysis of *Cellvibrio japonicus* xylanase 10C: how variation in substrate-binding cleft influences the catalytic profile of family GH-10 xylanases. J Biol Chem 2004;279:11777–11788.
10. Dominguez R, Souchon H, Spinelli S, Dauter Z, Wilson KS, Chauvaux S, Beguin P, Alzari PM. A common protein fold and similar active site in two distinct families of β-glycanases. Nat Struct Biol 1995;2:569–576.
11. Schmidt A, Schlacher A, Steiner W, Schwab H, Kratky C. Structure of the xylanase from *Penicillium simplicissimum*. Protein Sci 1998;7:2081–2088.
12. Schmidt A, Gubiz GM, Kratky C. Xylan binding subsite mapping in the xylanase from *Penicillium simplicissimum* using xylooligosaccharides as cryo-protectant. Biochemistry 1999;38:2403–2412.
13. Natesh R, Manikandan K, Bhanumoorthy P, Viswamitra MA, Ramakumar S. Thermostable xylanase from *Thermoascus Aurantiacus* at ultrahigh resolution (0.89A) at 100K and atomic resolution (1.11A) at 293K refined anisotropically to small-molecule accuracy. Acta Crystallogr D Biol Crystallogr 2003;59:105–117.
14. Lo Leggio L, Kalogiannis S, Eckert K, Teixeira SC, Bhat MK, Andrei C, Pickersgill RW, Larsen S. Substrate specificity and subsite mobility in *T. aurantiacus* xylanase 10A. FEBS Lett 2001;509:303–308.
15. Lo Leggio L, Kalogiannis S, Bhat MK, Pickersgill RW. High resolution structure and sequence of *T. aurantiacus* xylanase I: implications for the evolution of thermostability in family 10 xylanases and enzymes with (beta) alpha-barrel architecture. Proteins 1999;36:295–306.
16. Fujimoto Z, Kuno A, Kaneko S, Yoshida S, Kobayashi H, Kusakabe I, Mizuno H. Crystal structure of *Streptomyces olivaceoviridis* E-86 β-xylanase containing xylan-binding domain. J Mol Biol 2000;300:575–585.
17. Fujimoto Z, Kuno A, Kaneko S, Kobayashi H, Kusakabe I, Mizuno, H. Crystal structures of the sugar complexes of *Streptomyces olivaceoviridis* E-86 xylanase: sugar binding structure of family 13 carbohydrate-binding module. J Mol Biol 2002;316:65–78.
18. Fujimoto Z, Kaneko S, Kuno A, Kobayashi H, Kusakabe I, Mizuno H. Crystal structures of decorated xylooligosaccharides bound to a family 10 xylanase from *Streptomyces olivaceoviridis* E-86. J Biol Chem 2004;279:9606–9614.
19. Canals A, Vega MC, Gomis-Ruth FX, Diaz M, Santamaria RRI, Coll M. Structure of xylanase Xys1delta from *Streptomyces halstedii*. Acta Crystallogr D Biol Crystallogr 2003;59:1447–1453.
20. Teplitsky A, Mechaly A, Stojanoff V, Sainz G, Golan G, Feinberg H, Gilboa R, Reiland V, Zolotnitsky G, Shallom D, Thompson A, Shoham Y, Shoham G. Structure determination of the extracellular xylanase from *Geobacillus stearothermophilus* by selenomethionyl MAD phasing. Acta Crystallogr D Biol Crystallogr 2004;60: 836–848.
21. Zolotnitsky G, Cogan U, Adir N, Solomon V, Shoham G, Shoham Y. Mapping glycoside hydrolase substrate subsites by isothermal titration calorimetry. Proc Natl Acad Sci USA 2004;101:11275–11280.
22. Pell G, Taylor EJ, Gloster TM, Turkenburg JP, Fontes CM, Ferreira LM, Nagy T, Clark SJ, Davies GJ, Gilbert HJ. The mechanisms by which family 10 glycoside hydrolases bind decorated substrates. J Biol Chem 2004;279:9597–9605.
23. Payan F, Leone P, Porciero S, Furniss C, Tahir T, Williamson G, Durand A, Manzanares P, Gilbert HJ, Juge N, Roussel A. The dual nature of the wheat xylanase protein inhibitor XIP-I: structural basis for the inhibition of family 10 and family 11 xylanases. J Biol Chem 2004;279:36029–36037.
24. Winterhalter C, Liebl W. Two extremely thermostable xylanases of the hyperthermophilic bacterium *Thermotoga maritima* MSB8. Appl Environ Microbiol 1995;61:1810–1815.
25. Zhenqiang J, Kobayashi A, Ahsan MM, Lite L, Kitaoka M, Hayashi K. Characterization of a thermostable family 10 endoxylanase (XynB) from *Thermotoga maritima* that cleaves p-nitrophenol-β-D-xyloside. J Biosci Bioeng 2001;92:423–428.
26. Hakulinen N, Turunen O, Janis J, Leisola M, Rouvinen J. Three-dimensional structures of thermophilic beta-1,4-xylanases from *Chaetomium thermophilum* and *Nonomuraea flexuosa*. Comparison of twelve xylanases in relation to their thermal stability. Eur J Biochem 2003;270:1399–1412.
27. Ihsanawati, Kumasaka T, Kaneko T, Morokuma C, Nakamura S, Tanaka N. Crystallization and preliminary X-ray studies of xylanase 10B from *Thermotoga maritima*. Acta Crystallogr D Biol Crystallogr 2003;59:1659–1661.
28. Collaborative Computational Project, Number 4. Acta Crystallogr D Biol Crystallogr 1994;50:760–763.
29. Brünger A, Adams P, Clore G, DeLano W, Gros P, Grosse-Kunstleve R. Crystallography and NMR system: a new software suite for macromolecular structure determination. Acta Crystallogr D Biol Crystallogr 1998;54:905–921.
30. McRee DE. XtalView/Xfit: A versatile program for manipulating atomic coordinates and electron density. J Struct Biol 1999;125: 156–165.
31. Laskowski RA, MacArthur MW, Moss DS, Thornton JM. PROCHECK v.2.: Programs to check the stereochemistrial quality of protein structures, Oxford, UK: Oxford Molecular Ltd.; 1992.
32. Katapodis P, Vrsanska M, Kekos D, Nerinckx W, Biely P, Claeyssens M, Macris BJ, Christakopoulos P. Biochemical and catalytic properties of an endoxylanase purified from the culture filtrate of *Sporotrichum thermophile*. Carbohydr Res 2003;338:1881–1890.
33. Gasteiger E, Gattiker A, Hoogland C, Ivanyi I, Appel RD, Bairoch A. ExPASy: the proteomics server for in-depth protein knowledge and analysis. Nucleic Acids Res 2003;31:3784–3788.
34. Thompson JD, Higgins DG, Gibson TJ. CLUSTAL W: improving the sensitivity of progressive multiple sequence alignment through sequence weighting, position-specific gap penalties and weight matrix choice. Nucleic Acids Res 1994;22:4673–4680.
35. Kabsch W, Sander C. Dictionary of protein secondary structure: pattern recognition of hydrogen bonded and geometrical features. Biopolymers 1993;22:2577–2637.
36. Willard L, Ranjan A, Zhang H, Monzavi H, Boyko RF, Sykes BD, Wishart DS. VADAR: a web server for quantitative evaluation of protein structure quality. Nucleic Acids Res 2003;31:3316–3319.
37. Kleywegt GJ, Jones TA. Detection, delineation, measurement and display of cavities. Acta Crystallogr D Biol Crystallogr 1994;50: 178–185.
38. Kraulis, P. J., MOLSCRIPT: a program to produce both detailed and schematic plots of protein structures. J Appl Crystallogr 1991;24:946–950.
39. Merritt EA, Murphy MEP. Raster3D version 2.0: a program for photorealistic molecular graphics. Acta Crystallogr D Biol Crystallogr 1994;50:869–873.
40. Gouet P, Courcelle E, Stuart DI, Metoz F. ESPript: Multiple sequence alignments in PostScript. Bioinformatics 1999;15:305–308.
41. DeLano, WL. The PYMOL Molecular Graphics System on World Wide Web (http://www.pymol.org); 2002.
42. Banner DW, Bloomer AC, Petsko GA, Phillips DC, Pogson CI, Wilson IA, Corran, PH, Furth AJ, Milman JD, Offord RE, Priddle JD, Waley SG. Structure of chicken muscle triose phosphate isomerase determined crystallographically at 2.5 Å resolution using amino acid sequence data. Nature 1975;255:609–614.
43. Davies GJ, Wilson KS, Henrissat B. Nomenclature for sugar-binding subsites in glycoside hydrolases. Biochem J 1997;321:557–559.
44. Zhenqiang J, Deng W, Zhu YP, Li LT, Sheng YJ, Hayashi K. The recombinant xylanase B of *Thermotoga maritima* is highly xylan specific and produces exclusively xylobiose from xylans, a unique character for industrial applications. J Mol Catalys B: Enzymatic 2004;27:207–213.
45. Cambillau C, Claverie JM. Structural and genomic correlates of hyperthermostability. J Biol Chem 2000;275:32383–32386.

46. Suhre K, Claverie JM. Genomic correlates of hyperthermostability, an update. J Biol Chem 2003;278:17198–17202.
47. Watanabe K, Hata Y, Kizaki H, Katsube Y, Suzuki Y. The refined crystal structure of *Bacillus cereus* oligo-1,6-glucosidase at 2.0 Å resolution: structural characterization of proline-substitution sites for protein thermostabilization. J Mol Biol 269;1997:42–53.
48. Mallick P, Boutz DR, Eisenberg D, Yeates TO. Genomic evidence that the intracellular proteins of archaeal microbes contain disulfide bonds, Proc Natl Acad Sci USA 99;2002:9679–9684.
49. Auerbach G, Ostendorp R, Prade L, Korndorfer I, Dams T, Huber R, Jaenicke R. Lactate dehydrogenase from the hyperthermophilic bacterium *Thermotoga maritima*: the crystal structure at 2.1 A resolution reveals strategies for intrinsic protein stabilization. Structure 1998;6:769–781.
50. Burley SK, Petsko GA. Aromatic-aromatic interactions: a mechanism of protein structure stabilization. Science 1985;229:23–28.
51. Vieille C, Zeikus GJ. Hyperthermophilic enzymes: Sources, uses and molecular mechanisms for thermostability. Microbiol Mol Biol Rev 2001;65:1–43.
52. Tyndall JD, Sinchaikul S, Fothergill-Gilmore LA, Taylor P, Walkinshaw MD. Crystal structure of a thermostable lipase from *Bacillus stearothermophilus* P1. J Mol Biol 2002;323:859–869.
53. Li T, Sun F, Ji X, Feng Y, Rao Z. Structure based hyperthermostability of archaeal histone HPhA from *Pyrococcus horikoshii*. J Mol Biol 2003;325:1031–1037.
54. Olson CA, Spek EJ, Shi Z, Vologodskii A, Kallenbach NR. Cooperative helix stabilization by complex Arg-Glu salt bridges. Proteins 2001;44:123–132.
55. Leemhuis H, Rozeboom HJ, Dijkstra BW, Dijkhuizen L. Improved thermostability of *Bacillus circulans* cyclodextrin glycosyltransferase by the introduction of a salt bridge. Proteins 2004;54:128–134.
56. Yip KS, Stillman TJ, Britton KL, Artymiuk PJ, Baker PJ, Sedelnikova SE, Engel PC, Pasquo A, Chiaraluce R, Consalvi V. The structure of *Pyrococcus furiosus* gluatamate dehydrogenase reveals a key role for ion-pair networks in maintaining enzyme stability at extreme temperatures. Structure 1995;3:1147–1158.
57. Maes D, Zeelen JP, Thanki N, Beaucamp N, Alvarez M, Thi MH, Backmann J, Martial, JA, Wyns L, Jaenicke R, Wierenga RK. The crystal structure of triosephosphate isomerase (TIM) from *Thermotoga maritima*: a comparative thermostability structural analysis of ten different TIM structures. Proteins 1999;37:441–453.